Applied Physics Letters

RESEARCH ARTICLE | SEPTEMBER 19 2023

Origin of electrical noise near charge neutrality in dual gated graphene device

Special Collection: Electronic Noise: From Advanced Materials to Quantum Technologies

Aaryan Mehra ; Roshan Jesus Mathew; Chandan Kumar

Appl. Phys. Lett. 123, 123103 (2023)
https://doi.org/10.1063/5.0147446

Applied Physics Letters ARTICLE pubs.aip.org/aip/apl

Origin of electrical noise near charge neutrality in dual gated graphene device

Cite as: Appl. Phys. Lett. **123**, 123103 (2023); doi: 10.1063/5.0147446
Submitted: 22 February 2023 · Accepted: 18 August 2023 ·
Published Online: 19 September 2023

Aaryan Mehra, Roshan Jesus Mathew, and Chandan Kumar[a)]

AFFILIATIONS

Centre for Nano Science and Engineering, Indian Institute of Science, Bangalore 560012, India

Note: This paper is part of the APL Special Collection on Electronic Noise: From Advanced Materials to Quantum Technologies.
[a)]**Author to whom correspondence should be addressed:** kchandan@iisc.ac.in

ABSTRACT

This Letter investigates low frequency $1/f$ noise in an hBN encapsulated graphene device in a dual gated geometry. The noise study is performed as a function of top gate carrier density (n_{TG}) at different back gate density (n_{BG}). The noise at low n_{BG} is found to be independent of top gate carrier density. With increasing n_{BG}, noise value increases, and a noise peak is observed near charge inhomogeneity of the device. A further increase in n_{BG} leads to a decrease in noise magnitude. The shape of the noise is found to be closely related to a charge inhomogeneity region of the device. Moreover, the noise and conductivity data near charge neutrality show clear evidence of noise emanating from a combination of charge number and mobility fluctuation.

Graphene, a single sheet of carbon has emerged as one of the most promising candidates for the future device applications, which can supersede the silicon technology. However, graphene devices are very sensitive to disorder fluctuations, which lead to fluctuations in channel current.[1,2] Thus, quantifying the effect of the disorder becomes crucial for using the graphene based devices for practical applications. The low frequency $1/f$ noise technique has been used extensively to study the effect of various disorders like roughness and trap states in the substrate,[3] short and long range disorder,[4] metal contact to graphene,[5] charge inhomogeneity,[6] grain boundaries,[7] etc. The $1/f$ noise not only affects the low frequency <100 kHz, but its possible upconversion also affects the phase noise at higher frequency. Thus, understanding the noise spectrum in graphene devices becomes cardinal for technological applications.

However, even after more than a decade of extensive research, there is no consensus on the origin and mechanism of $1/f$ noise in graphene devices.[1,8–10] The noise study in graphene has been performed on both silicon[11,12] and hBN substrate.[8–10,13] The study reveals that the graphene devices on the hBN substrate show much smaller noise as compared to the graphene on a silicon substrate. The noise reduction in hBN encapsulated devices is associated with the better screening of graphene from the trap states in the silicon substrate and to a very smooth surface of hBN which is free of dangling bonds.[8–10,13] However, noise in hBN encapsulated graphene devices shows different shapes and magnitudes as a function of the carrier density.[8–10,13] Moreover, the noise magnitude varies from device to device and also depends on the type of encapsulating hBN—commercial hBN or NIMS hBN.[10] Furthermore, it is reported that the noise magnitude in hBN encapsulated graphene can be further reduced by adding an additional graphite gate.[10] Thus, there is an increasing evidence that the carrier number fluctuation is the major noise source in graphene devices both on silicon and hBN encapsulated devices. However, there are also evidences of noise stemming from mobility fluctuations as well. The claim is made on the basis of electron-beam irradiated graphene[11,14] on the silicon substrate and from non-monotonous variation of noise with a magnetic field in hBN encapsulated[15] and suspended[16] graphene devices.

In this Letter, we present a schematic study of low frequency $1/f$ noise in the hBN encapsulated graphene device in a dual gated geometry. We have performed noise study in a small region of graphene, which is underneath the top gate. The noise measurements are performed as a function of top gate carrier density (n_{TG}) at different back gate density (n_{BG}). We find that noise is small and almost independent of n_{TG} at small values of n_{BG}. With increasing n_{BG}, noise starts to increase and obtains a maximum value near $n_{BG} = 1.5 \times 10^{12}$ cm^{-2}. With the further increase in n_{BG}, the noise value decreases and becomes independent of n_{BG}. Moreover, our measurements show that the noise amplitude is minimum at the charge neutrality point (CNP), and it increases on both sides with electron and hole doping with its peak appearing close to the charge inhomogeneity of the device. Our

results show that noise in hBN encapsulated graphene can be tuned by nearly two orders of magnitude. Furthermore, our analysis of noise and channel conductivity provides a clear evidence of noise emanating from a combination of the charge number and mobility fluctuation.

The hBN encapsulated graphene device is fabricated by following the standard dry transfer technique.[17] In brief, a glass slide is prepared with a poly methyl methacrylate (PMMA) layer, and graphene is exfoliated on it. The hBN is exfoliated on a freshly cleaved highly p doped silicon wafer. The glass slide containing PMMA and graphene is loaded in a micro-manipulator, and graphene is transferred on hBN. This is followed by cleaning the stack of hBN/graphene in acetone followed by IPA cleaning. A standard electron beam lithography procedure is used to pattern contacts on the graphene heterostructure, followed by thermal evaporation of 5 nm chromium and 70 nm gold at the base pressure of 3×10^{-7} mbar. The device is annealed in vacuum for 3 h at 400 °C. To define the top gate, a thin top hBN is transferred on the hBN/graphene stack. This is followed by the final step where electron beam lithography is used to pattern the contacts, followed by metal deposition.

Figure 1(a) presents the schematic of our device along with the resistance measurement scheme. The optical image of the device is shown in supplementary material Fig. S1. All the measurements are performed at 77 K. The graphene is encapsulated between the top and bottom hBN. The carrier density in the device is tuned by the combination of top gate and back gate voltages. The thin top hBN and 300 nm thick SiO_2 act as the top and back gate dielectric, respectively. The back gate controls the density throughout the graphene channel while the top gate tunes the carrier density in a small portion of graphene, underneath the top gate. The total channel length and width are 8 and 2 μm, respectively. The distance between voltage probes is 4 μm, and the top gate width is 2 μm. Figure 1(b) shows the four probe conductivity data as a function of the top gate and back gate carrier density. A horizontal and diagonal stripe can be seen in the figure where the conductivity is minimum. The horizontal stripe corresponds to the Dirac point throughout the graphene channel, which is independent of the top gate carrier density while the diagonal stripe represents the Dirac cone in a small portion of graphene under the top gate region. Doping of carrier density (either electron or hole) leads to an increase in conductivity. This is shown explicitly in figure (c) and (d) by taking horizontal and vertical cut lines from Fig. 1(b), denoted by dashed arrows. We estimate the top hBN thickness to be ∼14 nm.

The low frequency noise is a versatile tool to study the effect of metal contact, charge fluctuation, screening, etc., on the device conductivity, which cannot be accessed by the traditional conductivity measurement methods.[1,2] It is characterized by normalized power spectral density, which is inversely proportional to the frequency, $S_V/V^2 \propto f^{-\beta}$, with $\beta = 1$. In most of the semiconducting devices, the noise power spectral density follows an empirical relation:[1,2]

$$S_V/V^2 = \alpha_H/Nf^{\beta}, \tag{1}$$

where S_V/V^2 is the normalized voltage noise density, f is the frequency, V is the bias voltage, N is the total number of charge carriers, and α_H is Hooge's parameter.

Figure 2(a) shows the normalized voltage noise density (S_V/V^2) at fixed n_{BG} for a few representative n_{eff}. The measurement setup is discussed in the supplementary material. A clear $1/f$ noise behavior with $\beta \approx 1$ can be seen from the figure. The noise value is quantified by calculating the noise amplitude (A), which is defined as[1]

$$A = \frac{1}{N}\sum_{n=1}^{N} f_n S_{Vn}/V_n^2. \tag{2}$$

Here, S_{Vn}/V_n^2 is the normalized noise spectral density at n different frequencies f_n. The other method to quantify the noise amplitude is to measure the normalized noise spectral density at a fixed frequency; however, this method is more prone to errors.[18]

Figures 2(b) and 2(c) show the noise amplitude as a function of the effective carrier density ($n_{eff} = n_{TG} - n_{Dirac}$) beneath the top gate for different values of n_{BG} with $n_{BG} > 0$. At low n_{BG} (close to the back gate Dirac point), the noise is almost independent of the effective carrier concentration. As the back gate density is increased, the noise amplitude starts increasing. The noise amplitude shows a clear "M" shape with effective density at $n_{BG} = 1.3 \times 10^{12}\text{cm}^{-2}$. With the further increase in n_{BG}, the noise amplitude increases and obtains a maximum peak value of $\approx 1.1 \times 10^{-7}$ at $n_{BG} = 1.5 \times 10^{12}\text{cm}^{-2}$. A further

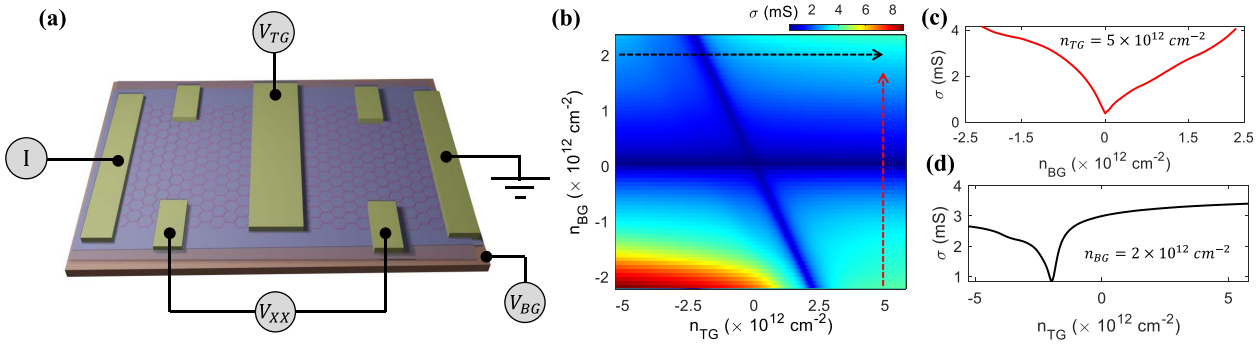

FIG. 1. (a) Schematic of the measured hBN encapsulated graphene device along with the resistance measurement scheme. The device is fabricated using the dry transfer technique.[17] The graphene is encapsulated between the top and bottom hBN with thickness ∼14 and ∼25 nm, respectively. The back gate controls the carrier density throughout the device while the top gate controls the carrier density only beneath the top gate region. (b) 2D color map of conductivity as a function of the top gate and back gate carrier density. The horizontal blue stripe shows the Dirac point throughout the device while the diagonal stripe shows the Dirac point from a small section of graphene underneath the top gate region. The vertical and horizontal cut line from panel (b) is presented in (c) and (d), respectively. As can be seen, the conductivity is minimum at the Dirac point and increases with electron or hole doping. All the measurements are performed at 77 K.

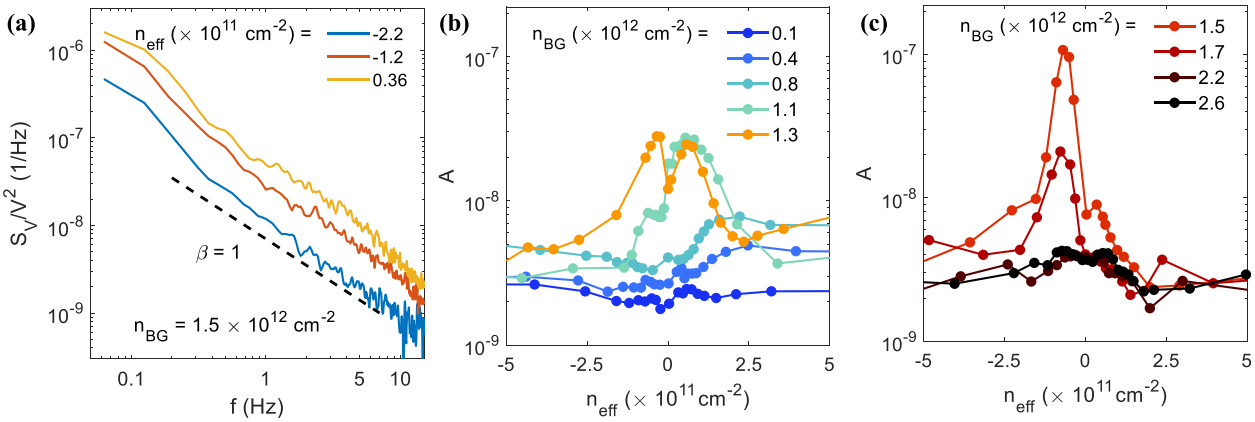

FIG. 2. (a) Normalized noise spectral density in the hBN encapsulated graphene device at few representative n_{eff} at $n_{BG} = 1.5 \times 10^{12}\text{cm}^{-2}$. The dashed line represents a pure $1/f$ line with $\beta = 1$. (b) and (c) Noise amplitude (A) as a function of the effective carrier density $n_{eff} = n_{TG} - n_{Dirac}$ underneath the top gate at different n_{BG}. At low n_{BG}, the noise amplitude is almost independent of n_{eff}. With increasing n_{BG}, noise increases and maximum noise is observed at $n_{BG} = 1.5 \times 10^{12}\text{cm}^{-2}$. The further increase in n_{BG} leads to reduction in the noise amplitude.

increase in n_{BG} leads to an overall decrease in the noise amplitude. Our measurements show a similar trend for negative values of n_{BG} (supplementary material Fig. S4). To elucidate the noise behavior with back gate carrier concentration, we plot the noise amplitude with n_{BG} in Fig. 3. It is obtained by finding the maximum noise amplitude value for different n_{BG} from Figs. 2(b), 2(c), and supplementary material Fig. S4.

The noise in graphene shows various shapes and noise magnitudes,[1,3,8–10,13,15,16,19–25] and they have been explained considering the charge number fluctuation or carrier mobility fluctuation model or the combination of both. According to the McWhorter charge number fluctuation model, the $1/f$ noise originates from charge trapping and detrapping events occurring between the channel and the trap states in gate oxides, which are located at different distances from the channel. The noise spectral density is written as[26]

$$S_I/I^2 = \frac{\lambda k T N_t}{f A V n^2}. \tag{3}$$

Here, λ is the tunneling constant, N_t is the trap concentration near Fermi energy, A is the gate area, and n is the carrier concentration in the device. It is important to note that our device has two different regions with different carrier concentrations—one underneath the top gate, where the density is controlled by the combination of the back gate and top gate and other where the density is determined only by the back gate. Although our measurements are performed as a function of the top gate carrier density, but since the voltage probes are present in the back gate region, the noise in our device can originate from a combination of back gate and top gate regions. Since n_{eff} is kept constant in the top gate region, the McWhorter charge number fluctuation models predict a decrease in noise with increasing n_{BG}, which is in stark contrast with our experimental results, which show non-monotonous density dependence (Fig. 3).

Recent years have seen increasing evidence of mobility fluctuation in graphene devices.[1,11,14–16] The mobility fluctuation model predicts that noise originates from the superposition of multiple events, which changes the scattering cross section σ. The power spectral density is given by[1,15,16]

$$S_I/I^2 \propto \frac{N_t^{\mu}}{V}\frac{\tau\zeta(1-\zeta)}{1+(\omega\tau)^2} l_0^2(\sigma_2-\sigma_1)^2, \tag{4}$$

where N_t^{μ} is the concentration of centers contributing to mobility fluctuation, τ is the characteristic time, $\zeta(1-\zeta)$ is the probability of with cross section $\sigma_1(1-\sigma)$, V is the volume of the sample, and l_0 is the mean free path. The model predicts that noise is directly proportional to N_t^{μ} and l_0^2. The mean free path (l_0) is calculated from the σ Vs n_{BG} curve, obtained from Fig. 1(a) by taking vertical cut at $n_{TG} = 0$ (the

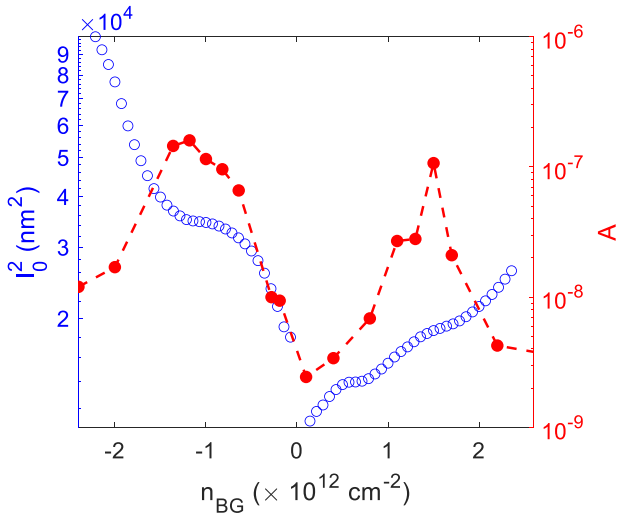

FIG. 3. Noise amplitude (A) and l_0^2 on right and left y axes, respectively, as a function of the back gate carrier density at fixed $n_{eff} \approx 1 \times 10^{11}\text{cm}^{-2}$. The noise amplitude is obtained by finding the maximum noise amplitude value for different n_{BG} from Figs. 2(b), 2(c), and supplementary material Fig. S4. The mean free path is obtained from σ Vs n_{BG} plot (supplementary material Fig. S2), obtained by taking vertical cut line at $n_{TG} = 0$ from Fig. 1(b). The noise is found to increase with increasing mean free path until a critical point beyond which noise decreases.

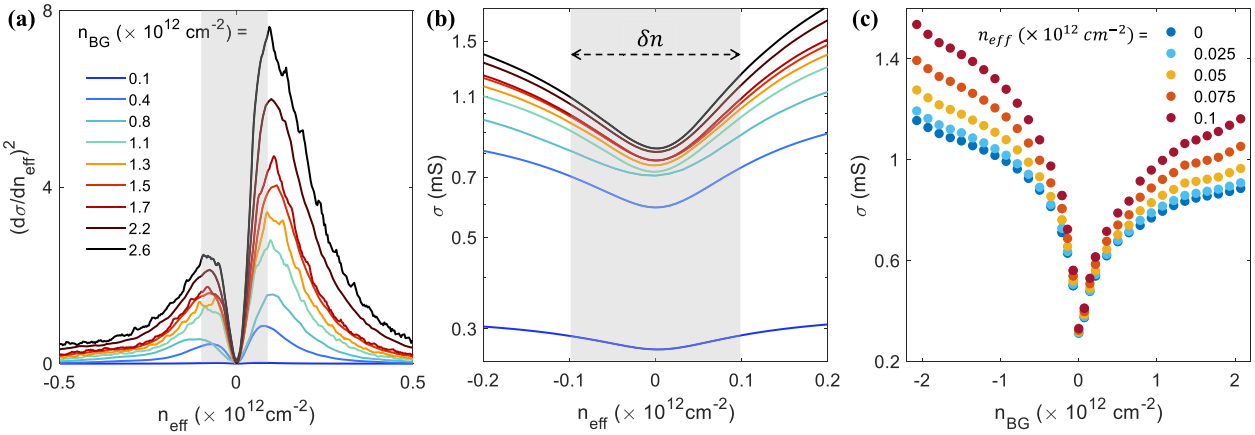

FIG. 4. (a) $(d\sigma/dn_{eff})^2$ as a function of the effective carrier density in the top gate region. The dip and peaks in $(d\sigma/dn_{eff})^2$ correspond to the Dirac point and charge inhomogeneity dn region underneath the top gate region. The estimated $\delta n \sim 1 \times 10^{11}\text{cm}^2$ is found to be independent of n_{BG}. The shaded region represents the δ_n region. (b) Conductivity as a function of the effective carrier density in the top gate region. The δn region is represented by the shaded gray region. An increase in conductivity is observed even in the δn region. (c) Conductivity as a function of n_{BG} at few representative points in the δn region, obtained by taking a vertical cut line from (b). A clear increase in conductivity is observed with n_{BG} even in the δn region.

supplementary material). The resultant l_0^2 is plotted in the left axis of Fig. 3. We find that the noise amplitude, A and l_0^2 increases with increasing n_{BG}, which is consistent with the mobility fluctuation model. However, beyond a critical l_0^2, noise starts to decrease. This can be due to a decrease in N_t^{μ}, which compensate the effect of increasing l_0^2. Similar results were also reported by Cultrera *et al.*[11]

Moreover, the enhanced mean free path throughout the device should also increase the conductivity in the top gated region. We plot $(d\sigma/dn_{eff})^2$ for different n_{BG} in Fig. 4(a). As can be seen from the figure, the charge inhomogeneity region is almost independent of n_{BG}, for $n_{BG} > 0.8 \times 10^{12}\,\text{cm}^{-2}$. We estimate $\delta n \approx 1 \times 10^{11}\,\text{cm}^{-2}$, and this is highlighted by gray stripe. In Fig. 4(b), we plot conductivity as a function of n_{eff} for different n_{BG} close to the Dirac point. We find an increase in conductivity even in the δn region. To highlight the same, we plot conductivity in the δn region as a function of n_{BG} in Fig. 4(c). It is obtained by taking vertical line traces from Fig. 4(b) in the δn region. A clear increase in conductivity is found in the δn region. However, by definition, the conductivity in the δn region should not change. The increase in conductivity in the δn region underneath the top gate can arise from an overall increase in the device mean free path (Fig. 3), which is consistent with the mobility fluctuation model.

To understand the shape and position of noise in Figs. 2(b) and 2(c), we plot the noise amplitude (A) and $(d\sigma/dn_{eff})^2$ as a function of n_{eff} for different set of back gate densities in Fig. 5 on right and left axes, respectively. The dip in $(d\sigma/dn_{eff})^2$ corresponds to the Dirac point, and the peaks correspond to the charge inhomogeneity (δn) of the graphene channel underneath the top gate We find that the noise minimum coincides with the Dirac point while the noise peak values are close to the charge inhomogeneity point of the graphene channel underneath the top gate (Fig. 5). Similar M shape noise behavior was also reported in hBN encapsulated graphene as a function of the back gate carrier density.[27] The charge inhomogeneity model of Xu *et al.*[28] can qualitatively explain the position of noise maximum in Figs. 5(a) and 5(c). In the charge inhomogeneity region, the noise amplitude can be written

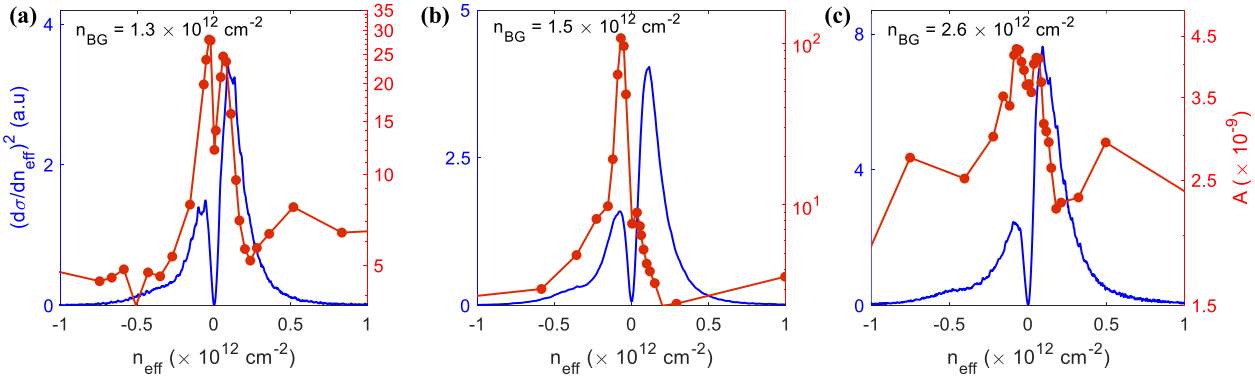

FIG. 5. (a)–(c) Noise amplitude (A) and $(d\sigma/dn_{eff})^2$ on right and left y axes, respectively, as a function of the effective carrier density at few representative n_{BG}. The dip in $(d\sigma/dn_{eff})^2$ corresponds to the Dirac point underneath the top gate region, and the peaks correspond to charge the inhomogeneity region, δn. We estimate $\delta n \sim 1 \times 10^{11}\text{cm}^{-2}$. The dip observed in noise corresponds to the Dirac point while the peaks in noise are near the δn.

as a combination of noise originating from the electron and hole charge puddles, i.e., $A \sim \alpha_H/(n_e D_e) + \alpha_H/(n_h D_h)$; here, n and D represent the density and puddle size, respectively, and subscript represents the electron–hole. Thus, electron doping in the channel will not only increase the electron density but will also increase the electron puddle size and decrease the hole puddle size. This leads to less noise due to electron charge carriers and large noise due to minority charge carriers leading to an increase in noise in the charge inhomogeneity region. With the further increase in the carrier density, the minority (hole) puddle size starts shrinking and can no longer contribute to the noise. Thus, beyond the δn region, main contribution to noise comes from majority (electron) carriers and, hence, noise decreases following the Hooges Empirical relation, $A \sim \alpha/N_e$. The disappearance of M shape noise in Fig. 5(b) can be due to spatial variation of charge inhomogeneity or Fermi energy fluctuation.[29]

In conclusion, our measurements have shown that various different noise shapes and noise magnitude reported to date in hBN encapsulated devices can be realized in a single graphene device by performing noise measurement in the dual gated geometry. Our results show that at low back gate density, noise is small and is almost independent of the effective carrier density. As the back gate density is increased, the noise magnitude increases by almost two orders of magnitude. With the further increase in the back gate density, the noise magnitude decreases. From our analysis, we trace the origin of noise emanating from a combination of the charge inhomogeneity and mobility fluctuation mechanism.

See the supplementary material for optical image of the device, mean free path calculation, $1/f$ noise measurement technique, and noise contribution from top gated and non-top-gated regions.

The authors gratefully acknowledge the National Nano Fabrication Centre (NNFC) and Micro and Nano Characterization Facility (MNCF) at the Center for Nano Science and Engineering (CeNSE), IISc for help and support in carrying out this work. The authors acknowledge funding support for CeNSE facilities from the Ministry of Human Resource Development (MHRD), Ministry of Electronics and Information Technology (MeitY), and Department of Science and Technology (DST). The authors thank Anindya Das for insightful discussion. C.K. acknowledges the IISc start up grant and QuRP seed fund grant for supporting this work.

AUTHOR DECLARATIONS

Conflict of Interest

The authors have no conflicts to disclose.

Author Contributions

Aaryan Mehra: Data curation (lead); Formal analysis (lead); Investigation (lead). **Roshan Jesus Mathew:** Formal analysis (equal); Investigation (equal). **Chandan Kumar:** Conceptualization (lead); Supervision (lead).

DATA AVAILABILITY

The data that support the findings of this study are available from the corresponding author upon reasonable request.

REFERENCES

[1]A. A. Balandin, "Low-frequency 1/f noise in graphene devices," Nat. Nanotechnol. **8**, 549–555 (2013).
[2]S. Islam, S. Shamim, and A. Ghosh, "Benchmarking noise and dephasing in emerging electrical materials for quantum technologies," Adv. Mater. **35**, 2109671 (2023).
[3]A. Kaverzin, A. S. Mayorov, A. Shytov, and D. Horsell, "Impurities as a source of 1/f noise in graphene," Phys. Rev. B **85**, 075435 (2012).
[4]Y. Zhang, E. E. Mendez, and X. Du, "Mobility-dependent low-frequency noise in graphene field-effect transistors," ACS Nano **5**, 8124–8130 (2011).
[5]P. Karnatak, T. P. Sai, S. Goswami, S. Ghatak, S. Kaushal, and A. Ghosh, "Current crowding mediated large contact noise in graphene field-effect transistors," Nat. Commun. **7**, 13703 (2016).
[6]I. Heller, S. Chatoor, J. Maannik, M. A. Zevenbergen, J. B. Oostinga, A. F. Morpurgo, C. Dekker, and S. G. Lemay, "Charge noise in graphene transistors," Nano Lett. **10**, 1563–1567 (2010).
[7]V. Kochat, C. S. Tiwary, T. Biswas, G. Ramalingam, K. Hsieh, K. Chattopadhyay, S. Raghavan, M. Jain, and A. Ghosh, "Magnitude and origin of electrical noise at individual grain boundaries in graphene," Nano Lett. **16**, 562–567 (2016).
[8]M. Kayyalha and Y. P. Chen, "Observation of reduced 1/f noise in graphene field effect transistors on boron nitride substrates," Appl. Phys. Lett. **107**, 113101 (2015).
[9]C. Kumar, M. Kuiri, J. Jung, T. Das, and A. Das, "Tunability of 1/f noise at multiple Dirac cones in hBN encapsulated graphene devices," Nano Lett. **16**, 1042–1049 (2016).
[10]S. Kakkar, P. Karnatak, M. A. Aamir, K. Watanabe, T. Taniguchi, and A. Ghosh, "Optimal architecture for ultralow noise graphene transistors at room temperature," Nanoscale **12**, 17762–17768 (2020).
[11]A. Cultrera, L. Callegaro, M. Marzano, M. Ortolano, and G. Amato, "Role of plasma-induced defects in the generation of 1/f noise in graphene," Appl. Phys. Lett. **112**, 093504 (2018).
[12]T. Wu, A. Alharbi, T. Taniguchi, K. Watanabe, and D. Shahrjerdi, "Low-frequency noise in irradiated graphene FETs," Appl. Phys. Lett. **113**, 193502 (2018).
[13]M. A. Stolyarov, G. Liu, S. L. Rumyantsev, M. Shur, and A. A. Balandin, "Suppression of 1/f noise in near-ballistic h-BN-graphene-h-BN heterostructure field-effect transistors," Appl. Phys. Lett. **107**, 023106 (2015).
[14]M. Zahid Hossain, S. Rumyantsev, M. S. Shur, and A. A. Balandin, "Reduction of 1/f noise in graphene after electron-beam irradiation," Appl. Phys. Lett. **102**, 153512 (2013).
[15]A. Rehman, J. A. D. Notario, J. S. Sanchez, Y. M. Meziani, G. Cywiński, W. Knap, A. A. Balandin, M. Levinshtein, and S. Rumyantsev, "Nature of the 1/f noise in graphene–direct evidence for the mobility fluctuation mechanism," Nanoscale **14**, 7242–7249 (2022).
[16]M. Kamada, W. Zeng, A. Laitinen, J. Sarkar, S.-S. Yeh, K. Tappura, H. Seppä, and P. Hakonen, "Suppression of $1/f$ noise in graphene due to non-scalar mobility fluctuations induced by impurity motion," arXiv:2112.11933 (2021).
[17]P. Zomer, S. Dash, N. Tombros, and B. van Wees, "A transfer technique for high mobility graphene devices on commercially available hexagonal boron nitride," Appl. Phys. Lett. **99**, 232104 (2011).
[18]Y.-M. Lin and P. Avouris, "Strong suppression of electrical noise in bilayer graphene nanodevices," Nano Lett. **8**, 2119–2125 (2008).
[19]M. A. Aamir and A. Ghosh, "Electrical noise inside the band gap of bilayer graphene," 2D Mater. **6**, 025018 (2019).
[20]M. Tian, Q. Hu, C. Gu, X. Xiong, Z. Zhang, X. Li, and Y. Wu, "Tunable 1/f noise in CVD Bernal-stacked bilayer graphene transistors," ACS Appl. Mater. Interfaces **12**, 17686–17690 (2020).
[21]G. Liu, S. Rumyantsev, M. S. Shur, and A. A. Balandin, "Origin of 1/f noise in graphene multilayers: Surface vs. volume," Appl. Phys. Lett. **102**, 093111 (2013).
[22]N. Mavredakis, R. G. Cortadella, A. B. Calia, J. A. Garrido, and D. Jiménez, "Understanding the bias dependence of low frequency noise in single layer graphene FETs," Nanoscale **10**, 14947–14956 (2018).
[23]S. Peng, Z. Jin, D. Zhang, J. Shi, D. Mao, S. Wang, and G. Yu, "Carrier-number-fluctuation induced ultralow 1/f noise level in top-gated graphene field effect transistor," ACS Appl. Mater. Interfaces **9**, 6661–6665 (2017).

[24]M. Kumar, A. Laitinen, D. Cox, and P. J. Hakonen, "Ultra low 1/f noise in suspended bilayer graphene," Appl. Phys. Lett. **106**, 263505 (2015).
[25]A. N. Pal, A. A. Bol, and A. Ghosh, "Large low-frequency resistance noise in chemical vapor deposited graphene," Appl. Phys. Lett. **97**, 133504 (2010).
[26]A. Dmitriev, M. Levinshtein, and S. Rumyantsev, "On the Hooge relation in semiconductors and metals," J. Appl. Phys. **106**, 024514 (2009).
[27]C. Kumar and A. Das, "Effect of boron nitride defects and charge inhomogeneity on 1/f noise in encapsulated graphene," Appl. Phys. Lett. **119**, 223106 (2021).
[28]G. Xu, C. M. Torres, Jr., Y. Zhang, F. Liu, E. B. Song, M. Wang, Y. Zhou, C. Zeng, and K. L. Wang, "Effect of spatial charge inhomogeneity on 1/f noise behavior in graphene," Nano Lett. **10**, 3312–3317 (2010).
[29]B. Pellegrini, "1/f noise in graphene," Eur. Phys. J. B **86**, 1–12 (2013).